Available online at www.sciencedirect.com
SCIENCE DIRECT®
Journal of Solid State Chemistry 172 (2003) 89–94
JOURNAL OF SOLID STATE CHEMISTRY
http://elsevier.com/locate/jssc

Cation and anion ordering in the layered oxyfluorides $Sr_{3-x}A_xAlO_4F$ (A = Ba, Ca)

A.K. Prodjosantoso,[a,b] B.J. Kennedy,[a,*] T. Vogt,[c] and P.M. Woodward[d]

[a] *Centre for Heavy Metals Research, School of Chemistry, The University of Sydney, Sydney, NSW 2006, Australia*
[b] *Jurusan Kimia, Universitas Negeri Yogyakarta, Yogyakarta DIY 55281, Indonesia*
[c] *Physics Department, Brookhaven National Laboratory, Upton NY 11973-5000, USA*
[d] *Chemistry Department, Ohio State University, Columbus, OH 43210-1185, USA*

Received 18 June 2002; received in revised form 21 October 2002; accepted 25 October 2002

Abstract

The synthesis and structural characterization of mixed oxyfluorides of the type $Sr_{3-x}A_xAlO_4F$ is reported, where A is either calcium or barium. In these compounds the fluoride and oxide ions are ordered onto two distinct crystallographic sites. There is also an ordering of the alkaline earth cations over two crystallographic sites upon substitution of Ba^{2+} or Ca^{2+} for Sr^{2+}. The solid solubility limits extend to $x \sim 1$ for substitution of both barium and calcium, but the larger Ba^{2+} cations show a strong site preference for the ten-coordinate strontium sites, while the smaller Ca^{2+} cations prefer the eight-coordinate strontium sites.

1. Introduction

The chemistry of mixed oxyfluorides is of considerable interest. The replacement of oxide by fluoride offers an attractive method of altering the charge within a system without dramatically altering the structure of the material due to the similar radii of the two anions. This approach has been used by Edwards et al. and others to tune the superconductivity in selected high T_c cuprates [1,2]. The replacement of oxygen by fluorine is also promising in the optimization of non-linear optical materials [3]. Despite the similarity of the two anions, there is an emerging body of evidence that F:O anion ordering can occur [4–8]. This can be difficult to determine since neither X-ray nor neutron diffraction measurements can reliably distinguish between oxygen and fluorine atoms, based on their scattering power.

Examples where F:O ordering is proposed include $Sr_2CuO_2F_{2+\delta}$, in which Edwards et al. observed that fluorine has a preference for the apical sites in the K_2NiF_4-type structure [1] and $BaMBO_3F_2$, M = Ga, Al, in which the F and O atoms are ordered in the axial and equatorial positions of MO_3F_2 bipyramids [4]. Similar ordering is present in the Ruddlesden Popper type layered materials $Sr_3Fe_2O_6F_{0.67}$ and Ba_2InO_3F [5,6].

We recently reported the synthesis and structure of the two novel layered oxyfluorides, Sr_3AlO_4F and Sr_3GaO_4F. These compounds contain Sr_2F sheets held together by isolated MO_4 tetrahedra and additional Sr^{2+} ions [9]. These compounds are isostructural with Sr_2EuAlO_5 and Sr_2GdGaO_5 in which ordering of the Sr and rare earth cations has been observed [10]. Since the coordination environment of the two strontium sites in these compounds are noticeably different, it is possible that cation ordering can be induced by replacing strontium with another alkaline earth ion, or possibly even a rare earth ion and alkali metal cation pair. The ease with which this substitution can occur will give an indication of prospects for the further synthesis of isostructural analogs. The site preferences of substitutional ions and the corresponding structural distortions that accompany these substitutions have implications for preparation of new optical materials, where doping with luminescent ions is required. Finally, both O/F anion ordering and ordering of electropositive isovalent cations are relatively uncommon. These compounds provide an unusual opportunity to study both types of ordering simultaneously.

*Corresponding author. Fax: +61-2-9351-3329.
E-mail address: kennedyb@chem.usyd.edu.au (B.J. Kennedy).

0022-4596/03/$ - see front matter © 2002 Elsevier Science (USA). All rights reserved.
doi:10.1016/S0022-4596(02)00128-7

2. Experimental

The samples of $Sr_{3-x}A_xAlO_4F$ (A = Ca, Ba; $x \leqslant 1$) were prepared by heating the appropriate amounts of $CaCO_3$ (Univar 99%), or $BaCO_3$ (BDH Analar 99%), $SrCO_3$ (Merck pa.), SrF_2 (Aldrich) and $Al(NO_3)_3\,9H_2O$ (Aldrich 98%) in air. The compounds formed after annealing treatments at 700°C, 800°C, and 900°C for 24 h each and then, after further grinding, they were finally annealed for 72 h at 1050°C and 1100°C for $Sr_{3-x}Ca_xAlO_4F$ and $Sr_{3-x}Ba_xAlO_4F$, respectively.

The synchrotron powder X-ray diffraction patterns were measured at the high-resolution diffractometer X7A on the National Synchrotron Light Source at Brookhaven National Laboratory at a wavelength of $\lambda = 0.89913$ Å (Ba series) or 0.7076 Å (Sr series). All data were analyzed by the Rietveld method, using the program RIETICA, operating on a PC [11]. In these analyses the observed profiles were modelled using a pseudo-Voigt function modified for the low angle asymmetry. The background was estimated by interpolation between up to 30 points.

Atomic coordinates and lattice parameters for Sr_3AlO_4F [9] in the tetragonal $I4/mcm$ space group were used as a starting model in the Rietveld analysis of $Sr_{3-x}M_xAlO_4F$. Initially, it was assumed that the cations were fully disordered with the Sr and Ca or Ba statistically occupying the 4*a* and 8*h* sites. The atomic coordinates and displacement parameters of the two types of atoms occupying a single site were constrained to be equal. Once the refinements had converged, the site occupancies were allowed to vary, assuming that both sites were fully occupied and the stoichiometry was maintained. Placing fluorine at the origin resulted in a satisfactory fit of the data to the model given in Table 1. The refined lattice parameters, atomic coordinates and site occupancies are listed in Table 1, while selected atomic distances and angles are listed in Table 2. The Rietveld refinement plot for a representative example is shown in Fig. 1.

3. Results

The compounds $Sr_{3-x}A_xAlO_4F$ ($0 \leqslant x \leqslant 1$) were prepared by the direct solid state reaction of an intimate mixture of $Al(NO_3)_3$, $A(CO_3)_2$ and SrF_2 at temperatures of up to 1100°C. Preparations using BaF_2 or CaF_2 as the source of fluoride gave identical products. Powder X-ray diffraction measurements collected using Cu$K\alpha$ radiation and a Siemens D5000 diffractometer did not reveal any obvious impurities for the samples with $x \leqslant 1$. For higher Ca contents, $x > 1$, variable amounts of a phase similar to $Sr_3Al_2O_6$ were observed in the patterns [12]. An unidentified second phase was observed when Ba contents higher than $x = 1$ were used. These highly doped materials were not investigated further. Energy dispersive X-ray analysis of selected samples showed acceptable agreement between the observed and expected cation stoichiometries. The observed F contents were typically lower than expected, with the typical F:Al ratio of 0.7–0.8. This is thought to be a consequence of two factors, namely the very low intensity of the F$K\alpha$ line in the EDA spectra and the mobility of fluorine during electron bombardment [13]. The present oxyfluorides are air stable and appear resistant to hydrolysis on contact with the moisture in the air.

Partial replacement of Sr by Ca in Sr_3AlO_4F resulted in a progressive shift in the positions of the various Bragg reflections to higher angles as the cell size decreased (see Table 1). This contraction, whilst smooth, was not isotropic, with the *c*-axis decreasing more

Table 1
Structural parameters for $Sr_{3-x}A_xAlO_4F$ obtained by Rietveld analysis of synchrotron X-ray diffraction patterns

$x=$	a (Å)	c (Å)	R_p	R_{wp}	n $A(1)$[a]	n $A(2)$[a]	B $A(1)$	B $A(2)$	$A(2)$ x	O x	O z
0.0	6.7822(1)	11.1437(2)	3.35	4.96	0	0	1.11(5)	0.77(2)	0.1696(1)	0.1418(5)	0.6496(3)
$M=$ Ba											
0.1	6.8066(1)	11.1455(2)	6.77	8.61	0.44(2)	0	0.80(2)	0.23(2)	0.1695(1)	0.1408(3)	0.6475(2)
0.2	6.8183(1)	11.1499(2)	6.29	7.98	0.88(2)	0	0.68(2)	0.21(1)	0.1694(1)	0.1403(3)	0.6474(2)
0.4	6.8454(2)	11.1600(3)	6.75	8.50	1.89(2)	0	0.52(2)	0.16(2)	0.1695(1)	0.1390(3)	0.6473(2)
0.5	6.8485(2)	11.1656(2)	5.69	7.13	2.24(2)	0	0.30(2)	0.01(2)	0.1692(1)	0.1389(4)	0.6467(3)
0.8	6.8847(2)	11.1862(4)	5.16	6.85	3.20(2)	0	−0.09(2)	−0.32(2)	0.1692(1)	0.1380(4)	0.6464(3)
1.0	6.9192(2)	11.2072(4)	6.03	8.37	3.80(2)	0.20(2)	−0.23(2)	−0.41(2)	0.1693(1)	0.1373(4)	0.6462(3)
$M=$ Ca											
0.2	6.7551(2)	11.1170(4)	6.40	8.18	0	1.7(3)	0.36(2)	0.29(1)	0.1697(2)	0.1469(6)	0.6497(4)
0.4	6.7309(5)	11.0854(9)	6.46	8.31	0	2.86(6)	0.22(1)	0.16(2)	0.1677(2)	0.1420(8)	0.6461(4)
0.6	6.7063(8)	11.0507(10)	6.32	8.01	0	3.37(9)	0.46(2)	0.39(1)	0.1682(2)	0.1385(6)	0.6446(7)
1.0	6.6517(5)	10.9443(9)	7.30	9.92	0	3.86(6)	0.41(1)	0.30(1)	0.1681(2)	0.1419(8)	0.6457(4)

The structures were refined in the tetragonal space group $I4/mcm$. In this space group the atomic positions are as follows: $A(1)$: 0, 0, $\frac{1}{4}$; $A(2)$: x, $x+\frac{1}{2}$, 0; Al: 0, $\frac{1}{2}$, $\frac{1}{4}$; F: 0, 0, 0; O: x, $x+\frac{1}{2}$, z.

[a] The full occupancy of the A(1) is 4 and of the A(2) sites is 8.

Table 2
Selected atomic distances (Å) and angles (deg) of $Sr_{3-x}Ba_xAlO_4F$

A = Ba	$Sr_{3-x}A_xAlO_4F$					
	$x=0.1$	$x=0.2$	$x=0.4$	$x=0.5$	$x=0.8$	$x=1.0$
$A(1)$–O ($\times 8$)	2.864(1)	2.868(2)	2.885(2)	2.890(2)	2.908(2)	2.922(2)
$A(1)$–F ($\times 2$)	2.7864(1)	2.7874(1)	2.7900(1)	2.7914(1)	2.7966(1)	2.8018(1)
$A(2)$–O ($\times 2$)	2.457(3)	2.462(3)	2.478(3)	2.478(3)	2.491(4)	2.502(4)
$A(2)$–O($\times 4$)	2.683(2)	2.686(3)	2.684(3)	2.678(3)	2.684(3)	2.688(3)
Mean $A(2)$–O	2.61(5)	2.61(5)	2.61(4)	2.61(4)	2.62(4)	2.63(4)
$A(2)$–F ($\times 2$)	2.5282(2)	2.5335(3)	2.5427(2)	2.5446(3)	2.5580(3)	2.5675(3)
Al–O ($\times 4$)	1.773(3)	1.775(3)	1.768(3)	1.771(3)	1.774(3)	1.776(4)
O–Al–O	114.6(1)	114.5(1)	114.9(1)	115.1(1)	115.2(1)	115.4(1)
O–Al–O	99.79(9)	99.9(2)	99.2(2)	98.7(2)	98.5(2)	98.1(3)
Mean O–Al–O	107.1(1)	107.2(2)	107.1(2)	106.9(2)	106.9(2)	106.8(2)
A = Ca	$x=0.0$	$x=0.2$	$x=0.4$	$x=0.6$	$x=1.0$	
$A(1)$–O ($\times 8$)	2.842(4)	2.841(3)	2.837(3)	2.836(5)	2.836(2)	
$A(1)$–F ($\times 2$)	2.7869(1)	2.7793(1)	2.7713(2)	2.7644(3)	2.7486(2)	
$A(2)$–O ($\times 2$)	2.460(4)	2.417(6)	2.430(6)	2.433(8)	2.340(4)	
$A(2)$–O ($\times 4$)	2.797(4)	2.715(5)	2.646(5)	2.613(7)	2.617(5)	
Mean $A(2)$–O	2.68(7)	2.61(6)	2.57(5)	2.55(4)	2.52(4)	
$A(2)$–F ($\times 2$)	2.5188(8)	2.509(5)	2.5054(6)	2.4947(7)	2.4747(5)	
Al–O ($\times 4$)	1.761(4)	1.792(6)	1.776(6)	1.756(8)	1.760(4)	
O–Al–O	113.7(2)	112.8(2)	114.9(2)	116.2(3)	113.1(2)	
O–Al–O	101.3(4)	103.1(4)	99.2(4)	96.8(5)	98.7(3)	
Mean O–Al–O	107.5(3)	107.7(3)	107.1(3)	106.5(4)	105.7(3)	

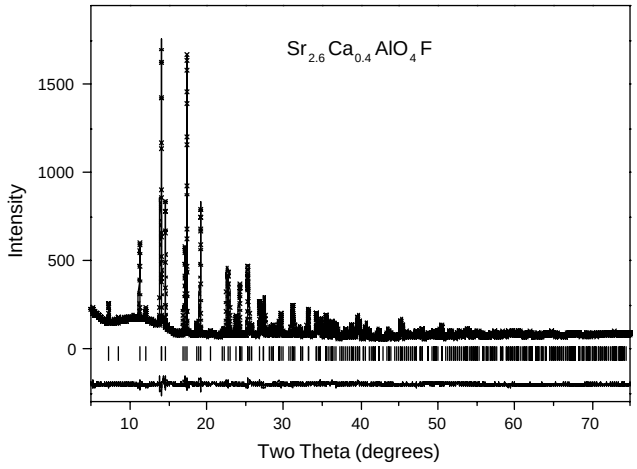

Fig. 1. Observed, calculated and difference synchrotron diffraction profiles for $Sr_{2.6}Ca_{0.4}AlO_4F$ recorded at $\lambda=07076$ Å. The short vertical lines indicate the positions of the allowed Bragg reflections.

rapidly. Conversely, substitution of the Sr by Ba resulted in a systematic increase in the cell size. The variations in lattice parameters were accurately fitted by simple quadratic functions. In both series, the variation in a is almost linear, as expected for a random distribution of the two A-type cations, whereas a marked curvature in the composition dependence of the c parameter was observed (see Fig. 2). Such a deviation from Vegard's Law is often observed when the cation distribution is not regular. Since Sr_3AlO_4F has a layered structure anisotropic expansion of the "in-plane" (ab) and axial (c) parameters is an indication that the cations are not randomly distributed [12]. This was confirmed in the structural refinements.

Results of the Rietveld refinements are summarized in Table 1. During the refinement stage, it was assumed that the fluorine was at the origin. Calculations of both bond valence sums and the Madelung site potentials demonstrate this assumption to be appropriate. The 4c Wyckoff site at the origin has a Madelung site potential of around 10 V, which is in the expected range for a fluoride ion, whereas the 16l Wyckoff site has a site potential near 20 V, typical of oxide ion site. The bond valence sums (BVS) of 1.28 and 2.02 for fluorine and oxygen, respectively, provide further evidence of an ordered anion distribution.

The larger A cations occupy two different sites. The $A(1)$ cation, which sits at Wyckoff site 4a, has a bicapped square antiprismatic coordination, with eight oxygens forming the square antiprism ($A(1)$–O distance is 2.842(4) Å in Sr_3AlO_4F) and two fluorines providing the capping ($A(1)$–F distance is 2.7869(1) Å in Sr_3AlO_4F). The $A(2)$ cation, which sits at Wyckoff site 8h, has a somewhat smaller and more distorted

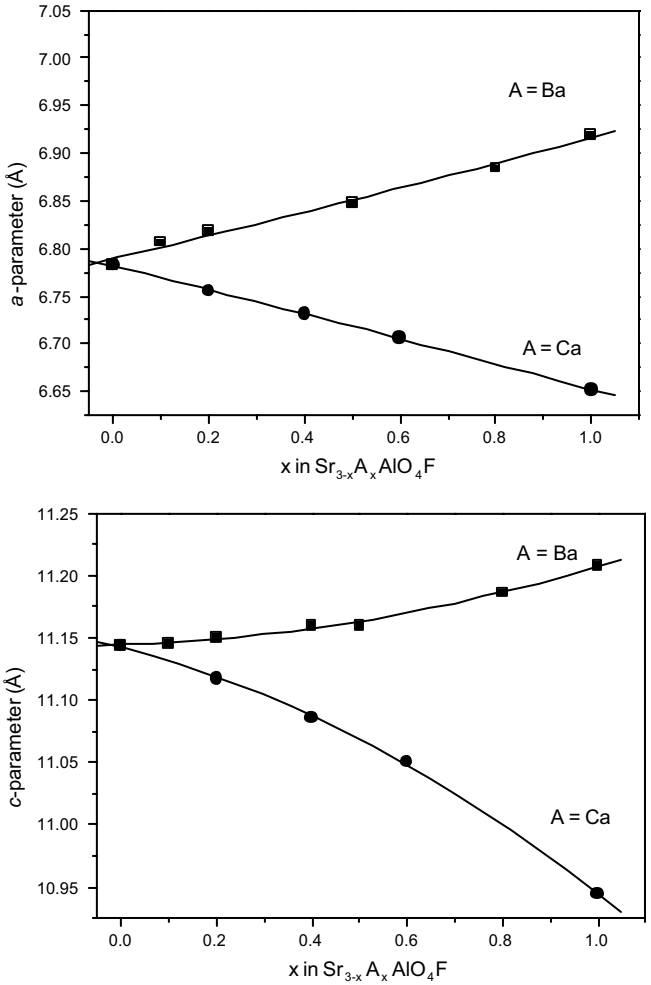

Fig. 2. Composition dependence of the tetragonal lattice parameters in the two series $Sr_{3-x}A_xAlO_4F$ (A = Ca or Ba).

coordination environment, with two fluorine ($A(2)$–F distance is 2.5188(8) Å in Sr_3AlO_4F) and six oxygen near neighbors ($A(2)$–O distances are $2 \times 2.460(4)$ Å and $4 \times 2.797(4)$ Å in Sr_3AlO_4F). Both coordination environments are illustrated in Fig. 3d. The refined occupancies of the two sites are listed in Table 1. In general, these are unremarkable. There is a noticeable reduction in the isotropic displacement parameters in the series $Sr_{3-x}Ba_xAlO_4F$ as the Ba content increases and this is presumably a consequence of absorption effects. A neutron diffraction study of the cation ordering may be informative. The structural refinements show that the smaller Ca ions preferentially occupy the $A(2)$ sites, whilst the larger Ba ions preferentially occupy the $A(1)$ sites. In the series $Sr_{3-x}Ca_xAlO_4F$ ($0 \leqslant x \leqslant 1$) only the $A(2)$ sites contains any Ca. Likewise in the series $Sr_{3-x}Ba_xAlO_4F$, only when $x > 0.8$ is any Ba observed in the $A(2)$ sites, as shown in Fig. 4.

4. Discussion

The results clearly show that in $Sr_{3-x}A_xAlO_4F$ both the anions and the alkaline earth cations preferentially order onto distinct crystallographic sites. To better understand the reasons for and implications of this ordering, let us consider the crystal structure more carefully. One way to visualize this structure is to deconstruct it into $A(2)_2F$ layers separated by a checkerboard arrangement of AlO_4 tetrahedra and $A(1)$ cations, as shown in Fig. 3a. Alternatively, one can describe the structure as an ABX_3 antiperovskite, sometimes observed for metal-rich carbides and nitrides such as $MgCNi_3$ [14] and $CuNMn_3$ [15]. In the antiperovskite description, the F^- ions occupy the octahedral site, the Sr^{2+} ions occupy the bridging X-sites (anion sites in an oxide or halide perovskite), and the AlO_4^{5-} ions occupy the A-site. The structure is drawn so as to emphasize this deconstruction in Fig. 3b. The aristotype antiperovskite structure is cubic, space group symmetry $Pm\bar{3}m$, but here the symmetry is lowered by two distortions of the FSr_3 framework: an axial elongation of the octahedra, and rotations of the octahedra about the c-axis. The axial elongation can clearly be seen in the parent compound, Sr_3AlO_4F, from the Sr–F distances. The axial F–Sr(1) distance is 2.7869(1) Å, while the equatorial F–Sr(2) distance is 2.5188(8) Å. In Sr_3AlO_4F, the octahedra are rotated by $\sim 18^\circ$ about the c-axis. The direction of the rotation alternates from one layer to the next. This pattern of octahedral rotations is classified as $a^0a^0c^-$ in the notation of Glazer [16] or $00\phi_z$ in the notation of Aleksandrov [17]. Fig. 3c shows how both the axial elongation and the octahedral rotations are necessary to accommodate the non-spherical AlO_4^{5-} tetrahedra on the A-site.

The calculated BVS for Sr_3AlO_4F and the substituted compounds are listed in Table 3. In Sr_3AlO_4F, the BVS for the Sr^{2+} ion on the $A(2)$ site is close to the expected value, but the Sr^{2+} ion on the $A(1)$ site is dramatically underbonded. Thus it is easy to understand the strong preference of the larger Ba^{2+} ion for the $A(1)$ site. In Sr_2BaAlO_4F where the Sr^{2+} and Ba^{2+} ions are almost completely ordered, the BVS values indicate that Sr^{2+} is ideally sized for the $A(2)$ site and Ba^{2+} is a good fit for the $A(1)$ site. Table 3 also shows that Ba^{2+} ions located on the $A(2)$ site would be significantly overbonded. This view of the structure is consistent with the solubility limit of $x = 1$ in $Sr_{3-x}Ba_xAlO_4F$.

While the bond valence analysis shows $BaSr_2AlO_4F$ to be a stable composition, the very low BVS value for Sr^{2+} in Sr_3AlO_4F makes one wonder how the parent compound maintains its thermodynamic stability. Perhaps the $A(1)$ ions simply compensate charge within a fairly rigid framework formed from the AlO_4 tetrahedra and the $A(2)_2F$ layers, and the undersized Sr^{2+} ions are

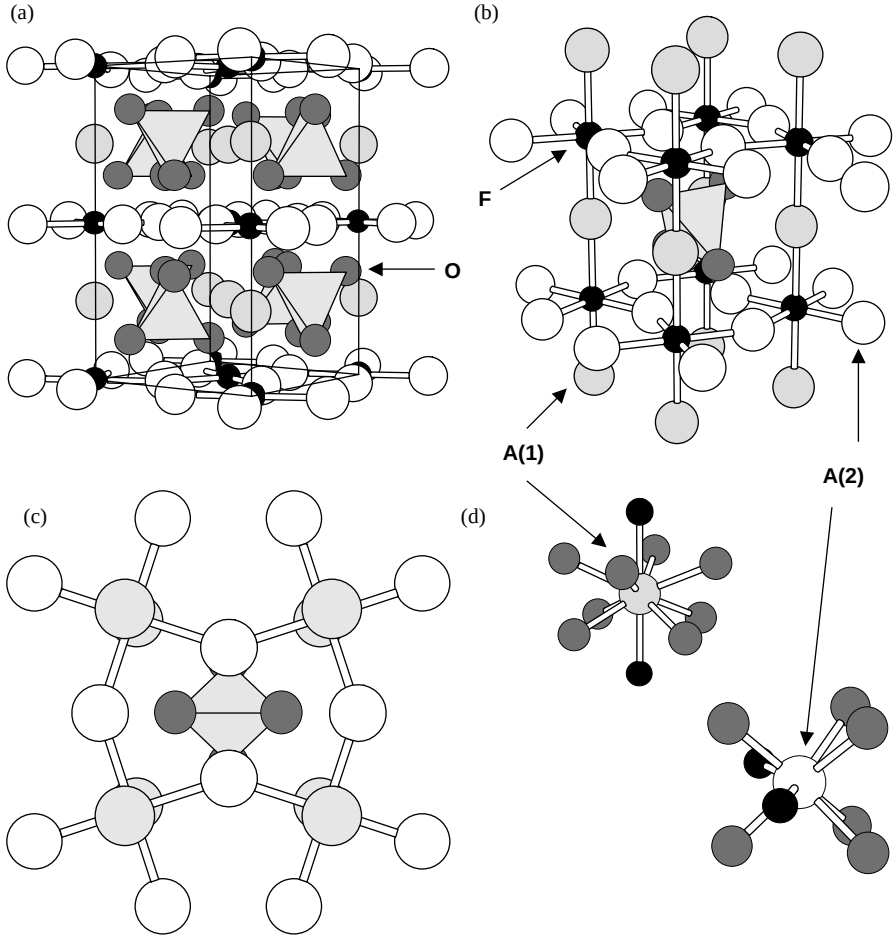

Fig. 3. The structure of M_3AlO_4F revealing: (a) the stacked $M(2)_2F$ layers at $z = 0$ and $\frac{1}{2}$ which are separated by isolated AlO_4 tetrahedra and $A(1)$ ions, (b) a comparison to a distorted antiperovskite where the F ions are octahedrally coordinated and the AlO_4^{5-} tetrahedra act as the A cations, (c) the tilting distortion of the FA_3 network is driven by the orientation of the AlO_4^{5-} tetrahedra in order to optimize the $A(2)$–O distances, and (d) the coordination environment of the $A(1)$ and $A(2)$ ions.

left to rattle in their oversized cavities. One observation that supports this view of the structure is the structural response to Ba^{2+} substitution, where the $A(1)$–O and $A(1)$–F distances change by a relatively small amount upon replacement of Sr^{2+} with the much larger Ba^{2+} ion.

The bond valence analysis can also be used to rationalize the strong preference of the smaller Ca^{2+} ion for the $A(2)$ site. Following the logic of the proceeding paragraphs, one would expect that the solid solubility limit should extend up to $x = 2$ ($SrCa_2AlO_4F$). However, in practice, we were only able to substitute up to $x \cong 1$ before secondary phases began to appear. The reason for this is not immediately apparent. It could be that the structure only tolerates the size mismatch between Sr^{2+} and Ca^{2+} up to a certain point. The A–F bonding may also play a role. The two $A(2)$–F contacts only contribute roughly $\frac{1}{4}$ of the total valence of the $A(2)$ cation, while interactions with oxygen provide the remaining $\sim 75\%$. Therefore, substitution of Ca^{2+} for Sr^{2+} on the $A(2)$ site necessarily triggers a contraction of the c-axis in order to generate shorter $A(2)$–O distances. This in turn leads to a contraction of the $A(1)$–F distances. However, the bond valence calculations show that fluorine is already overbonded. Therefore, the $A(1)$–F interaction may ultimately limit the contraction of the c-axis and in turn the solubility of Ca^{2+}.

5. Conclusions

Two series of isostructural compounds of the type $Sr_{3-x}M_xAlO_4F$ (M = Ca and Ba, $x \leqslant 1$) were synthesized and their structures analyzed using powder X-ray diffraction methods. The solid solubility limits extend to $x \sim 1$ for substitution of both barium and calcium for strontium. The structure are characterized by both F:O

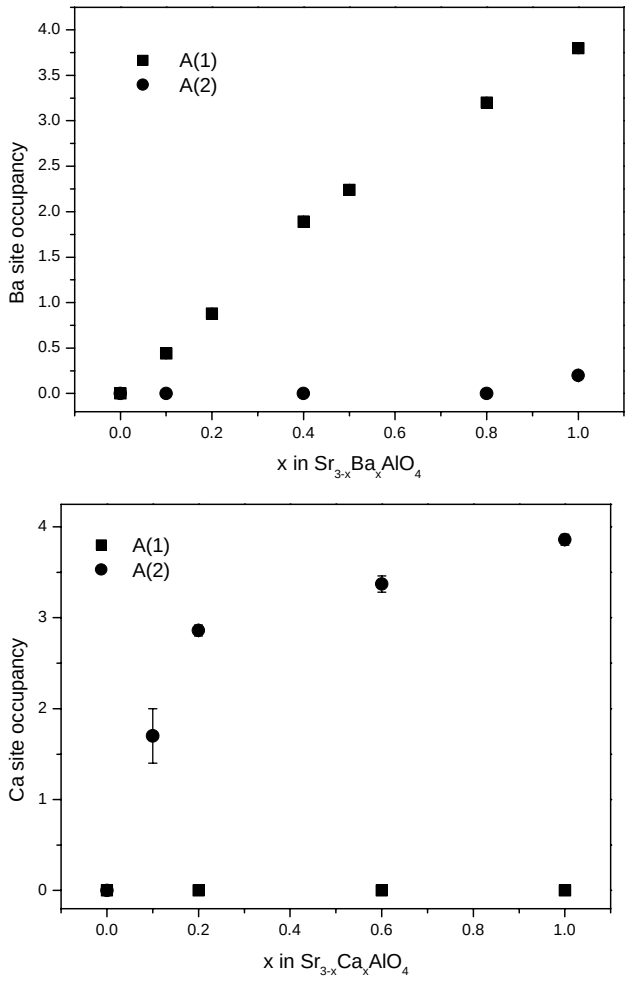

Fig. 4. Composition dependence of the site occupancies in the two series $Sr_{3-x}A_xAlO_4F$ (A = Ca or Ba).

ordering and alkaline earth cation ordering. The cations are not randomly distributed over these two sites, rather the larger Ba^{2+} cations show a strong preference for the ten-coordinate $A(1)$ sites and the smaller Ca^{2+} cations prefer the eight-coordinate $A(2)$ sites. The stability of the structures to these substitutions suggests that a wide range of cations may also be accommodated within this framework.

Acknowledgments

Work at Brookhaven is supported by the US Department of Energy, Division of Materials Sciences under Contract No. DE-AC02-98CH10886.

Table 3
Cation valence bond sums of selected cations of $Sr_{3-x}A_xAlO_4F$

Atoms	$Sr_{3-x}Ca_xAlO_4F$					
x	0	0.2	0.4	0.6	1	
Sr(1)	1.37	1.46	1.40	1.37	1.51	
Sr(2)	1.92	2.20	2.33	2.42	2.69	
		2.17[a]	**2.21**	**2.19**	**2.17**	
Ca(2)		1.45	1.54	1.61	1.78	
Al	2.73	2.51	2.62	2.77	2.74	
	$Sr_{3-x}Ba_xAlO_4F$					
x	0.1	0.2	0.4	0.5	0.8	1
Sr(1)	1.30	1.29	1.24	1.23	1.18	1.14
	1.39	**1.35**	**1.36**	**1.36**	**1.36**	**1.35**
Ba(1)	2.07	2.05	1.97	1.95	1.87	1.81
Sr(2)	2.14	2.12	2.08	2.09	2.04	1.99
					2.04	**2.01**
Ba(2)					3.24	3.18
Al	2.65	2.63	2.68	2.66	2.64	2.62

[a] Bold typed figures indicate average values obtained using the refined site occupancies.

References

[1] M. Al-Mamouri, P.P. Edwards, C. Greaves, M. Slaski, Nature 369 (1994) 382.
[2] M.G. Francesconi, P.R. Slater, J.P. Hodges, C. Graves, P.P. Edwards, M. Al-Mamouri, M. Slaski, J. Solid State Chem. 135 (1998) 17.
[3] L.F. Schneemeyer, L. Guterman, T. Siegrist, G.R. Kowach, J. Solid State Chem. 160 (2001) 333.
[4] H. Park, J. Barbier, J. Solid State Chem. 155 (2001) 354.
[5] R.L. Needs, M.T. Weller, J. Chem. Soc. Dalton Trans. 3015 (1995).
[6] G.S. Case, A.L. Hector, W. Levason, R.L. Needs, M.F. Thomas, M.T. Weller, J. Mater. Chem. 9 (1999) 2821.
[7] G. Cobel, R. Retoux, M. Leblanc, J. Solid State Chem. 139 (1998) 52.
[8] L.S. Du, F. Wang, C.P. Grey, J. Solid State Chem. 140 (1998) 285.
[9] T. Vogt, P.M. Woodward, B.A. Hunter, A.K. Prodjosantoso, B.J. Kennedy, J. Solid State Chem. 144 (1999) 228.
[10] J. Nguyen-Trut-Dinh, G. Fava, Le Flem, Z. Anorg. Allg. Chem. 433 (1997) 275.
[11] B.A. Hunter, C.J. Howard, A Computer Program for the Rietveld Analysis of X-ray and Neutron Powder Diffraction Patterns, 1996.
[12] A.K. Prodjosantoso, B.J. Kennedy, B.A. Hunter, Aust. J. Chem. 53 (2000) 195.
[13] J.C. Stormer, M.L. Pierson, Am. Minerol. 78 (1993) 641.
[14] T. He, Q. Huang, A.P. Ramirez, Y. Wang, K.A. Regan, N. Rogado, M.A. Hayward, M.K. Haas, J.S. Slusky, K. Inumara, H.W. Zandbergen, N.P. Ong, R.J. Cava, Nature 411 (2001) 54.
[15] E.O. Chi, W.S. Kim, N.H. Hur, Solid State Commun. 120 (2001) 307.
[16] A.M. Glazer, Acta Crystallogr. B 28 (1972) 3384.
[17] K.S. Aleksandrov, Kristallografiya 21 (1976) 249.